REGULAR ARTICLE

blood advances

Genome-wide promoter methylation of hairy cell leukemia

Alberto J. Arribas,[1,2,*] Andrea Rinaldi,[1,*] Giorgia Chiodin,[3] Ivo Kwee,[1,2,4] Afua Adjeiwaa Mensah,[1] Luciano Cascione,[1,2,5] Davide Rossi,[1,5] Meena Kanduri,[6] Richard Rosenquist,[7] Emanuele Zucca,[5] Peter W. Johnson,[3] Gianluca Gaidano,[8] Christopher C. Oakes,[9] Francesco Bertoni,[1] and Francesco Forconi[3,10,11]

[1]Università della Svizzera Italiana, Institute of Oncology Research, Bellinzona, Switzerland; [2]SIB Swiss Institute of Bioinformatics, Lausanne, Switzerland; [3]Cancer Sciences Unit, Cancer Research UK and NIHR Experimental Cancer Medicine Centres, University of Southampton, Southampton, United Kingdom; [4]Dalle Molle Institute for Artificial Intelligence, Manno, Switzerland; [5]Oncology Institute of Southern Switzerland, Bellinzona, Switzerland; [6]Department of Clinical Chemistry and Transfusion Medicine, Sahlgrenska University Hospital, Göteborg, Sweden; [7]Department of Molecular Medicine and Surgery, Karolinska Institute, Stockholm, Sweden; [8]Division of Haematology, Department of Translational Medicine, Amedeo Avogadro University of Eastern Piedmont, Novara, Italy; [9]Division of Hematology, Department of Internal Medicine, The Ohio State University, Columbus, OH; [10]Department of Medicine, Surgery, and Neuroscience, University of Siena, Siena, Italy; and [11]Haematology Department, Cancer Care, Southampton University Hospital Trust, Southampton, United Kingdom

Key Points

- Correspondence of normal B-cell subsets to HCL suggests the nontumoral counterpart of the disease.
- We identified a methylation-driven signature of HCL that involves genes regulating the B-cell receptor and the BRAF signaling pathways.

Classic hairy cell leukemia (HCL) is a tumor of mature clonal B cells with unique genetic, morphologic, and phenotypic features. DNA methylation profiling has provided a new tier of investigation to gain insight into the origin and behavior of B-cell malignancies; however, the methylation profile of HCL has not been specifically investigated. DNA methylation profiling was analyzed with the Infinium HumanMethylation27 array in 41 mature B-cell tumors, including 11 HCL, 7 splenic marginal zone lymphomas (SMZLs), and chronic lymphocytic leukemia with an unmutated (n = 7) or mutated (n = 6) immunoglobulin gene heavy chain variable (IGHV) region or using IGHV3-21 (n = 10). Methylation profiles of nontumor B-cell subsets and gene expression profiling data were obtained from public databases. HCL had a methylation signature distinct from each B-cell tumor entity, including the closest entity, SMZL. Comparison with normal B-cell subsets revealed the strongest similarity with postgerminal center (GC) B cells and a clear separation from pre-GC and GC cellular programs. Comparison of the integrated analysis with post-GC B cells revealed significant hypomethylation and overexpression of BCR–TLR–NF-κB and BRAF-MAPK signaling pathways and cell adhesion, as well as hypermethylation and underexpression of cell-differentiation markers and methylated genes in cancer, suggesting regulation of the transformed hairy cells through specific components of the B-cell receptor and the BRAF signaling pathways. Our data identify a specific methylation profile of HCL, which may help to distinguish it from other mature B-cell tumors.

Introduction

Classic hairy cell leukemia (HCL) is a rare mature B-cell tumor that is characterized by the accumulation of leukemic cells in the bone marrow, spleen, and peripheral blood.[1]

The universal genetic fingerprint of HCL is the acquisition of the BRAF V600E mutation in all individual hairy cells.[1-5] The mutation leads to constitutive BRAF–MEK–ERK pathway activation[1,2] and represents an effective therapeutic target in patients.[3,6] KLF2 and CDKN1B (p27) mutations may cooperate with BRAF V600E in the tumor cells of some patients.[7] However, HCL typically has a highly stable genomic profile,[8,9] and the inability of BRAF inhibitors to completely eradicate HCL in patients suggests that factors other than genetics may contribute to disease pathogenesis and behavior.[2]

Submitted 1 August 2018; accepted 2 January 2019. DOI 10.1182/bloodadvances.2018024059.

*A.J.A. and A.R. contributed equally to the study.

The full-text version of this article contains a data supplement.

Expression of multiple functional immunoglobulin isotypes is another unique feature of HCL.[10,11] Its association with low levels of intraclonal variations of the immunoglobulin gene heavy chain variable (IGHV) region and ongoing isotype-switch events prior to deletional recombination are suggestive of ongoing environmental interactions promoting or maintaining the tumor clone.[12-15] However, the behavior of mature B-cell tumors is also influenced by the DNA methylation status of the transformed cell.[16-18] DNA methylation is involved in controlling cellular differentiation and cell type specification during hematopoietic development.[17,19] In the most common form of adult leukemia, chronic lymphocytic leukemia (CLL), the methylation profile is clearly different between the 2 main subsets with unmutated (U-CLL) or mutated IGHV (M-CLL) and is stable over the course of the disease, likely reflecting the maturation of the cell of origin.[17,20-22] Methylation profiling also helps to better define specific disease subentities, like IGHV3-21$^+$ CLL, and it can contribute to defining of disease prognosis.[17,23,24]

The DNA methylation profile of HCL has not been extensively investigated. Here, we investigated the DNA methylation profiles of a series of HCL using the Illumina HumanMethylation27 array and compared them with other B-cell tumor entities and with normal peripheral blood B cells at different stages of differentiation.

Methods

Tumor panel

Peripheral blood mononucleated cells were obtained at diagnosis or prior to any treatment from 41 mature B-cell tumors, including 11 HCLs, 7 splenic marginal zone (MGZ) lymphomas (SMZLs), 7 U-CLLs, and 6 M-CLLs. The CLL cohort also included 10 IGHV3-21$^+$ CLLs (CLL–VH3-21, all mutated for IGHV), which was analyzed as a separate subentity. Diagnosis was made according to the World Health Organization 2018 Classification of Tumors of Hematopoietic and Lymphoid Tissues.[25] Differential diagnosis of HCL and SMZL was verified by allele-specific oligonucleotide polymerase chain reaction and sequencing.[26] HCL samples were confirmed BRAF V600E mutated, whereas all SMZLs were confirmed BRAF V600E unmutated. Use and mutational status of the expressed tumor *IGHV* gene were determined using our previously reported procedures.[15] Purity of tumor B cells was ≥70% in all samples, as measured by immunophenotyping.[8] The characteristics of the 11 HCL samples are shown in supplemental Table 1. Patients provided informed consent in accordance with the local institutional review board requirements and the Declaration of Helsinki.

Genome-wide promoter methylation profiling

DNA extraction and quality control were performed as previously described.[8] Methylation profiling was performed with the Infinium HumanMethylation27 array (Illumina, San Diego, CA), as previously described.[27]

Data mining

Probes inside or outside cytosine guanine dinucleotide islands (CGIs)[28] were analyzed separately, as previously reported.[27] The methylation profiles of the CLL cases were derived from previous publications.[23,27] To identify the normal counterpart of HCL, defined as the nontumor B-cell subset with the closest methylation profile to HCL cells, we studied a series of B-cell subpopulations obtained with the Infinium HumanMethylation450 BeadChip and acquired from the European Genome-phenome Archive dataset EGAS00001000534.[18] Methylation data were preprocessed, including background correction and quantile normalization, using the "minfi" package in R environment.[29] Batch effect was corrected for 27k and 450k platforms using the ComBat algorithm,[30] and only probes commonly annotated in both 27k and 450k platforms were considered in the study. To stabilize the variance of methylation range across the series, β values were transformed into M-values for the identification of differentially methylated probes. A moderated Student *t* test (limma) was used to identify the differentially methylated regions (q value < 0.05; absolute difference of average M-values > 1.0).[31] To further identify probes with changes in methylation, the Fisher's exact test was performed on the β values ($P < .05$; not methylated for β from 0 to 0.33, hemimethylated for β from 0.33 to 0.66, and methylated for $\beta > 0.66$).

Gene expression profiling (GEP) data, obtained with Affymetrix U95A and U95Av2 arrays, were extracted from Gene Expression dataset GSE2350[32] and analyzed by limma to characterize the differentially expressed genes (q value < 0.05 and absolute $\log_2$ fold change >1.0). The methylation–GEP correlation (Pearson) was calculated only for genes with probes common to the GSE2350 dataset.[32] We considered inversely correlated those genes significantly hypomethylated and overexpressed, or hypermethylated and underexpressed, in ≥1 of the following independent comparisons (computed separately on methylation and gene expression profiles using the moderated Student *t* test): HCL vs post–germinal center (GC) B cells, HCL vs SMZL, HCL vs M-CLL, and HCL vs U-CLL. For functional annotation, >6100 gene sets belonging to The Molecular Signatures Database v5.1 gene set enrichment analysis (GSEA) collection,[33] were grouped into 100 major biological themes ("concepts," supplemental Table 2), reducing the number and the redundancy of gene sets. Single-sample GSEA ([ssGSEA], "GSVA" package in R environment)[34] was then performed on the methylation and GEP data. The ssGSEA output was subsequently analyzed by limma at the concepts level.[31] Analyses were performed using R environment (R Studio console; RStudio, Boston, MA).

Results

The global methylation pattern of HCL shows similarities to normal post-GC B-cell subsets and splenic MGZ B-cell lymphomas

We studied the genome-wide promoter methylation profile of 11 HCLs (all harboring BRAF V600E mutation) vs defined normal B-cell subsets[18,35] or vs SMZL (n = 7), U-CLL (n = 7), or M-CLL (n = 6).

Unsupervised analysis of all probes provided insight into the potential normal B-cell counterpart of HCL. Unsupervised clustering (Figure 1A) and multidimensional analysis (Figure 1B) highlighted a marked distance of HCL from naive B-cell and GC founder B-cell subsets, whereas the closest subsets to HCL were the post-GC subsets, including splenic MGZ, low-maturity memory, and intermediate-maturity memory B-cell subsets.

When the other B-cell tumors were compared, HCL samples clustered very much closer to SMZL than to CLL. Although the latter distributed largely according to its IGHV mutational status (U-CLL, M-CLL, IGHV3-21 CLL), as expected,[16,18,24] SMZL cases

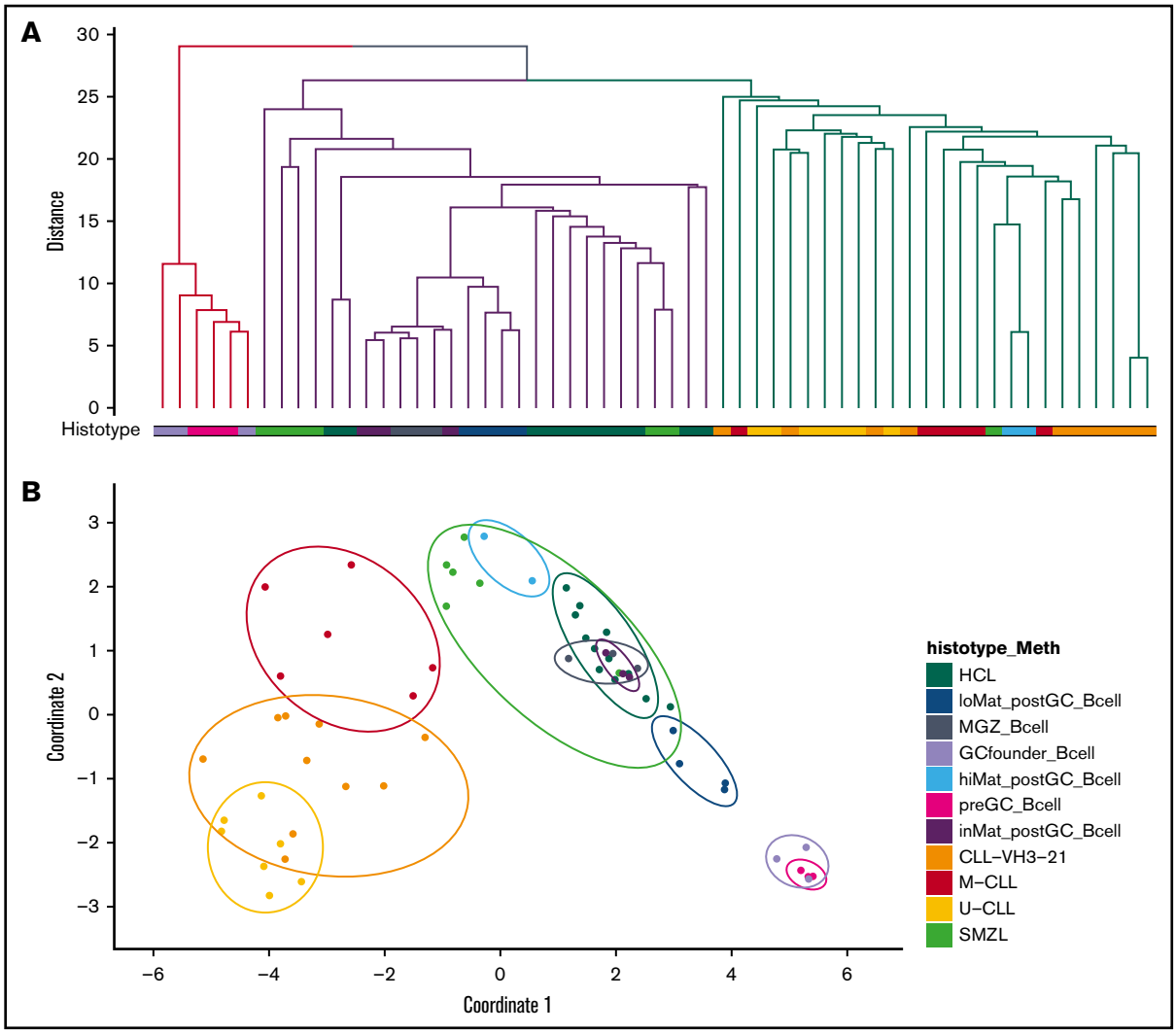

Figure 1. The global methylation pattern of HCL differs from other indolent B-cell tumors and normal B-cell subpopulations. (A) Unsupervised hierarchical clustering (Euclidean distance, complete linkage). (B) Multidimensional scaling plot showing a 2-dimensional projection of distances across the different histotypes within the series. Methylation profiling (histotype_Meth) included HCL, naive B cells (preGC_Bcell), GC founder B cells (B cells upon antigen encountering, GCfounder_Bcell), low-, intermediate-, and high-maturity memory B cells (loMat_postGC_Bcell, inMat_postGC_Bcell, and hiMat_postGC_Bcell, respectively), splenic MGZ B cells (MGZ_Bcell), CLL samples (U-CLL IGHV, M-CLL IGHV, IGHV3-21$^+$ [CLL–VH3-21]), and SMZL.

clustered with (2/7) or very close to (5/7) HCL samples. Indeed, 1 of the 2 cases, initially classified as CD103$^+$DBA44$^+$ HCL, lacked the BRAF V600E mutation and was reclassified as an SMZL only after central immunohistochemical revision due to ANXA-1 negativity.

Two additional unsupervised analyses were performed to better understand the epigenetic program of HCL cells: 1 for the CGI probes only (supplemental Figure 1A) and another 1 with probes outside of the CGIs (supplemental Figure 1B). Both analyses generally overlapped with the clustering on the global genome-wide methylation profile, although it is worth mentioning that the CGI-only methylation profile clustered all HCL samples in an independent branch, separately from post-GC B cells but still together with the 2 SMZL cases mentioned above.

Hence, this analysis documented that HCL has a global methylation profile close to post-GC B cells and SMZLs.

Methylation contributes to the HCL gene expression signature

HCL has a gene expression profile similar to that of post-GC B cells but with a specific signature that is distinct from normal and other neoplastic B cells.[32] The published HCL gene-expression signature[32] was then integrated with promoter methylation profiles by independent comparisons of HCL with post-GC B cells and with other B-cell tumors (HCL vs SMZL, HCL vs M-CLL, and HCL vs U-CLL). Enrichment analysis by GSEA revealed hypermethylation of the underexpressed HCL gene signature, whereas the overexpressed HCL signature was hypomethylated compared with post-GC B cells (supplemental Figure 2A). An integrated analysis using the moderated Student *t* test showed that 47% (36/76) of the differentially transcribed genes were inversely correlated with their methylation status (supplemental Figure 2B; supplemental Table 3). The top 10

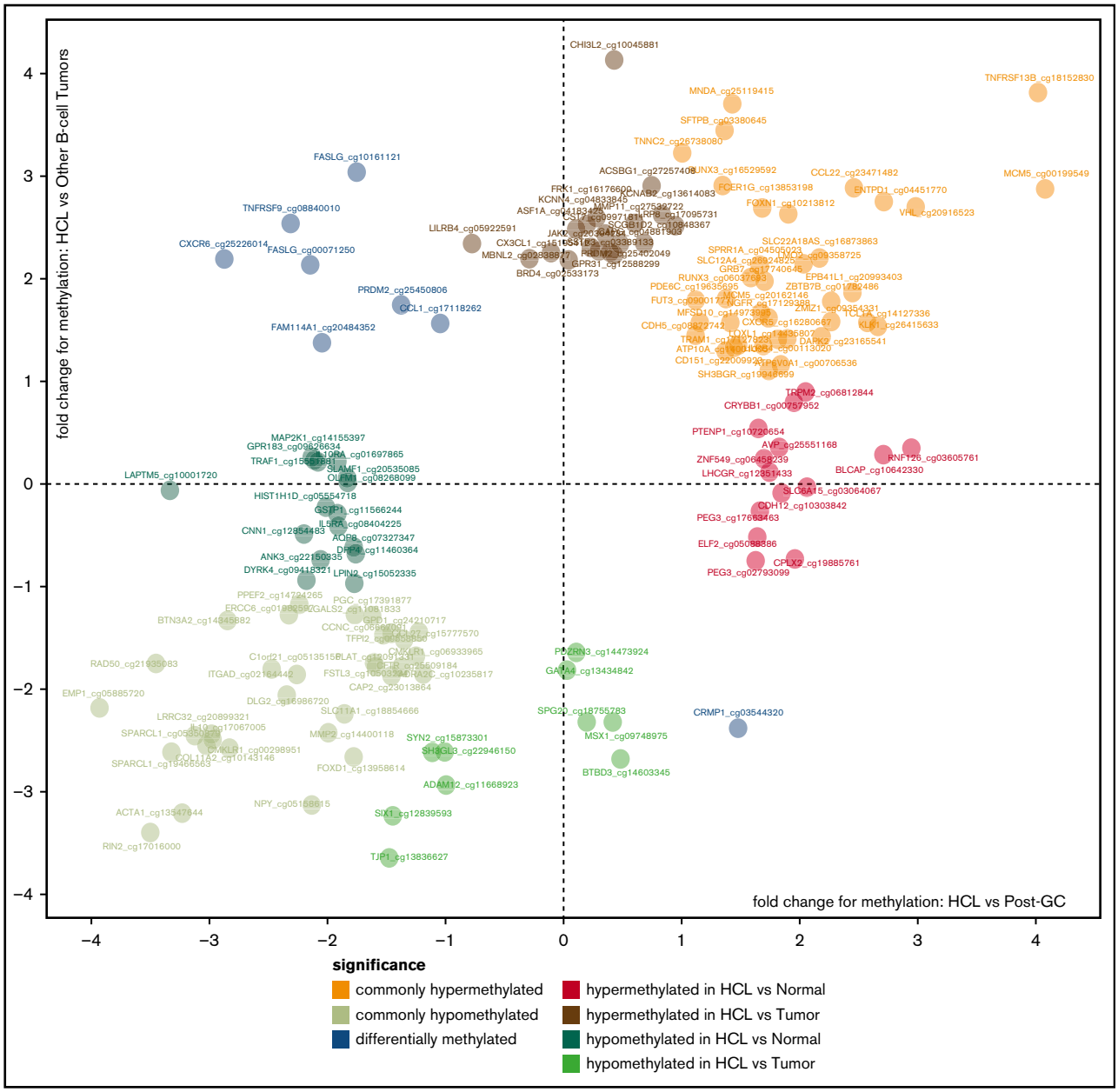

Figure 2. Integration of methylation profiles of HCL, post-GC B cells, and other B-cell tumors. Scatter plot on the differentially methylated probes (q value < 0.05; absolute difference of average M-values > 1.0). Fold change of HCL compared with post-GC B cells is shown on the x-axis, whereas the y-axis represents the fold change in HCL compared with other B-cell tumors, including SMZL and CLL. Commonly hypermethylated probes in HCL are highlighted in orange, whereas commonly hypomethylated probes are represented in lime green. Probes showing different methylation profile in HCL compared with post-GC B cells or with other B-cell tumors are in blue. Hypermethylated probes in HCL compared with normal or tumor are showed in red or brown, respectively, whereas hypomethylated probes in HCL vs post-GC B cells or other B-cell tumors are in green or light green, respectively. Labels show gene symbol and probe-ID by Illumina.

hypomethylated and overexpressed transcripts were *EPB41L2*, *DST*, *RIN2*, *EMP1*, *PDE4DIP*, *ENG*, *RCBTB2*, *AIF1*, *FLT3*, and *PLOD2*, whereas only 4 transcripts were hypermethylated and underexpressed: *CXCR5*, *TRAF5*, *PAWR*, and *TNFAIP8.*

The observed inverse correlation between gene expression and methylation (Pearson correlation $\rho = -0.375$, $P < .001$) points to DNA promoter methylation as a mechanism involved in the regulation of the specific gene expression signature of HCL.

Epigenetic profile identifies specific methylation patterns in HCL

Independent supervised analyses were performed to compare HCL methylation patterns with those of post-GC B cells and with the methylation profiles of SMZL, M-CLL, U-CLL, and CLL–VH3-21.

Commonly hypermethylated genes in HCL, compared with post-GC B cells or with the other B-cell tumors, included those involved in regulation of B-cell proliferation, cell motility, and immune system

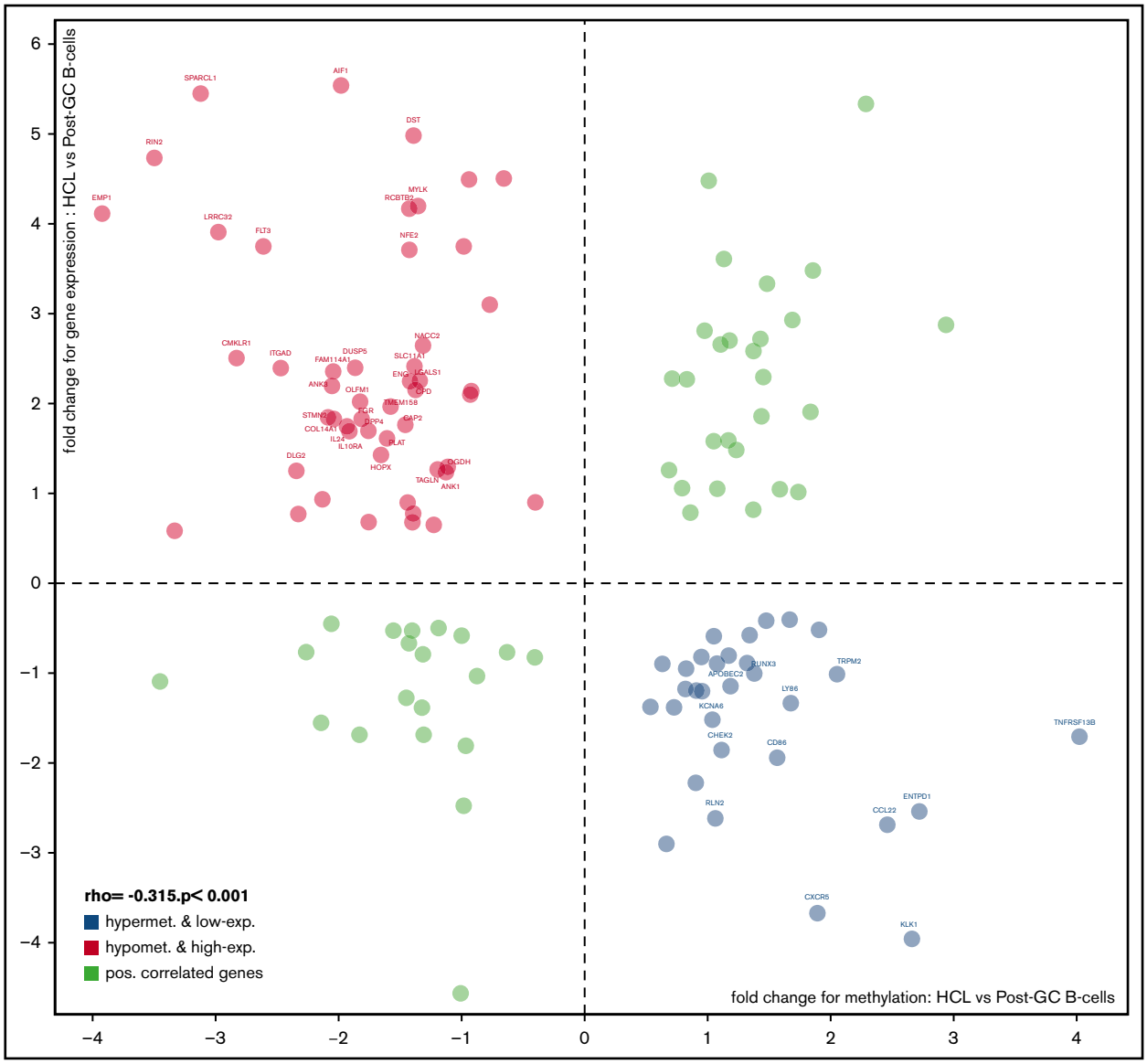

Figure 3. Integration of methylation and gene expression profiles of HCL and post-GC B cells. Scatter plot on the differentially methylated or expressed genes (q value < 0.05; absolute difference in average M-values > 1.0 for methylation, and absolute $\log_2$ fold change >1.0 for gene expression). Δ of M-value is represented on the x-axis, whereas the y-axis represents $\log_2$ fold change in gene expression. Negatively correlated genes are labeled and highlighted in blue (hypermethylated and underexpressed) or in red (hypomethylated and overexpressed), whereas positively correlated genes are not labeled and are represented in light green. The ρ and P values correspond to Pearson's correlation for methylation and GEP fold changes.

process. The top hypermethylated genes in HCL included *TNFRSF13B*, *MCM5*, *VHL*, *ENTPD1 (CD39)*, *CCL22*, *MNDA*, *SFTPB*, *FOXN1*, *FCER1G*, and *RUNX3.* Commonly hypomethylated genes included those involved in the RAS signaling cascade. The top 10 hypomethylated genes in HCL were *RIN2*, *ACTA1*, *EMP1*, *SPARCL1*, *COL11A2*, *IL10*, *LRRC32*, *CMKLR1*, *RAD50*, and *FOXD1* (Figure 2; supplemental Tables 4-10).

We then searched methylation differences between HCL and post-GC B cells for genes that were not differentially methylated from other B-cell tumors. Hypermethylated genes in HCL were annotated for transmembrane transport and genes downregulated by overexpression of an oncogenic form of KRAS; among the top genes we found *RNF126*, *BLCAP*, *CDH12*, *ELF2*, and *PTENP1.* The top hypomethylated genes in HCL were *LAPTM5*, *TRAF1*, *MAP2K1*, *IL10RA*, and *IL5RA*; and GSEA provided enrichment in antigen-dependent B-cell activation and RAS, interleukin-10 (IL-10), IL-2, and MAPK signaling pathways (Figure 2; supplemental Tables 4-10).

DNA promoter methylome of HCL was further interrogated to identify genes differentially methylated from other B-cell tumors (SMZL, M-CLL, U-CLL, and CLL–VH3-21) but not from post-GC B cells. Among the top hypermethylated genes we found *CHI3L2*, *MMP11*, *LILRB4*, *PRDM2 (RIZ1)*, and *BRD4*, whereas *TJP1*, *SIX1*, *ADAM12*, *BTBD3*, and *GATA4* were the top hypomethylated genes. GSEA showed that hypermethylated probes were enriched in genes modulated by AKT-mTOR, IL-2, and IL-15 signals and by

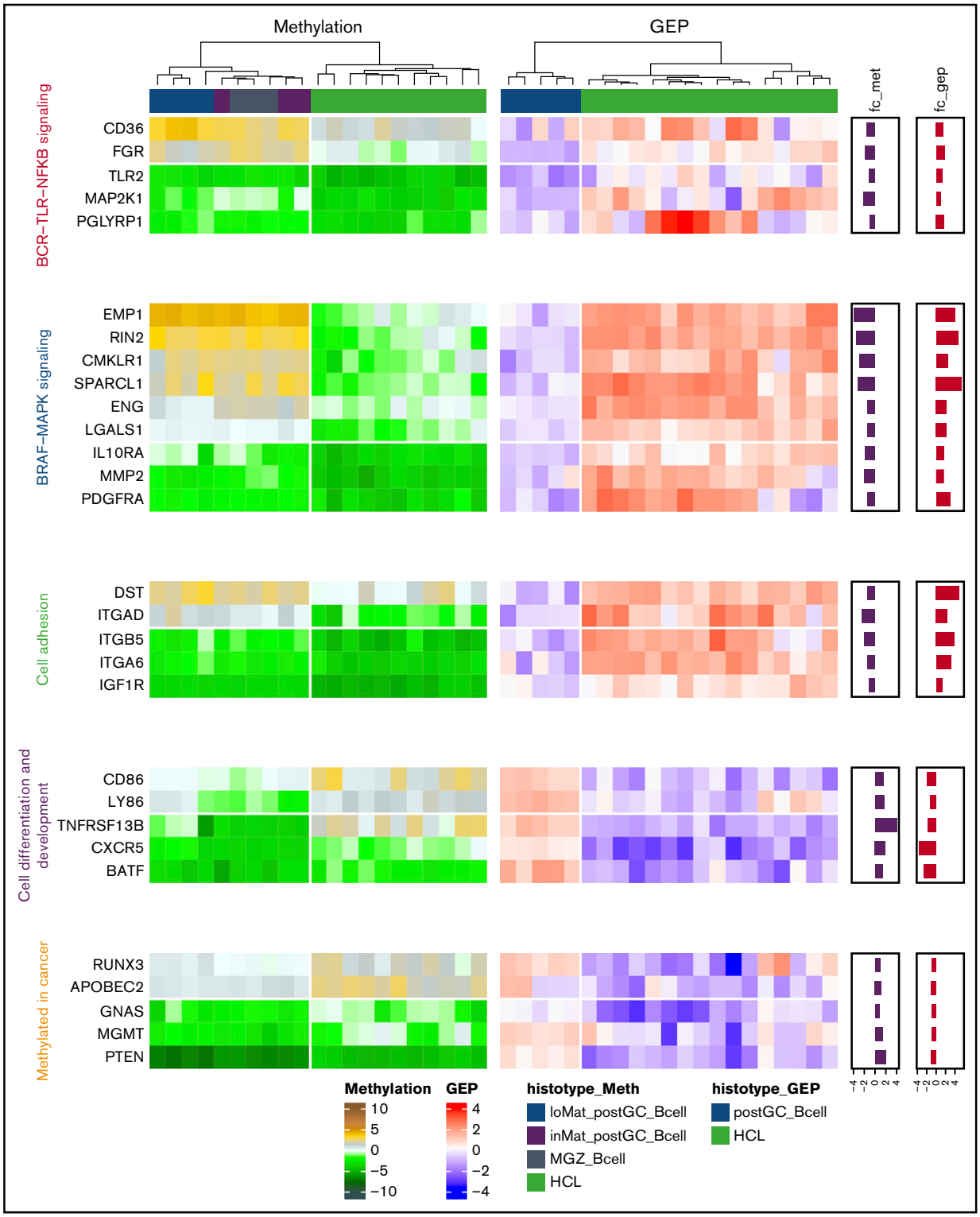

Figure 4. Differences in BCR–TLR–NF-κB or BRAF-MAPK pathway–associated gene methylation and expression for HCL and post-GC B cells. Integrated methylation (heat map on the left) and gene expression (heat map on the right) profiles of HCL and post-GC B cells revealed enrichment of transcripts annotated for BCR–TLR–NF-κB (red) or BRAF-MAPK (blue) signaling pathways and cell adhesion (green) among the hypomethylated and upregulated genes, whereas cell-differentiation markers (purple) and genes methylated in cancer (orange) were enriched among the hypermethylated and underexpressed transcripts. All selected genes showed statistically significant changes. *fc_met* (purple bars) represents fold change in methylation between HCL and post-GC B cells, and *fc_gep* (red bars) represents fold change in gene expression between HCL and post-GC B cells. Methylation profiling (histotype_Meth) included low- and intermediate-maturity memory B cells (loMat_postGC_Bcell and inMat_postGC_Bcell), splenic MGZ B cells (MGZ_Bcell), and HCL. GEP (histotype_GEP) included memory B cells (postGC_Bcell) and HCL.

JNK inhibitors; meanwhile, polycomb repressive complex 2 targets, cell–cell interactions, and G protein–coupled receptor signaling were enriched in the hypomethylated genes in HCL (Figure 2; supplemental Tables 4-10).

BCR–TLR–NF-κB and BRAF-MAPK pathway methylation and expression patterns differ in HCL and post-GC B cells

Methylation and gene expression profiles were further integrated to compare HCL with post-GC B-cell subsets. The unsupervised methylation profiling analysis identified low-maturity memory and intermediate-maturity memory B cells and MGZ B cells as the normal populations closest to HCL; unfortunately, gene expression data for these populations were not publicly available.[32] Thus, we integrated the methylation profile of post-GC B cells (nonclass switched and class switched) with the gene expression profile of the closest available B-cell subset, $CD27^+$ memory B cells, although these were primarily represented by class-switched memory B cells.

Despite this shortcoming, the comparison identified 119 hypermethylated or hypomethylated genes in HCL. *TNFRSF13B*, *ENTPD1*, *KLK1*, *CCL22*, *TRPM2*, *CXCR5*, *LY86*, *CD86*, *RUNX3*, and *APOBEC2* were the 10 most hypermethylated and underexpressed genes, whereas the top 10 genes with hypomethylation and high expression included *SPARCL1*, *RIN2*, *EMP1*, *LRRC32*, *AIF1*, *FLT3*, *CMKLR1*, *DST*, *RCBTB2*, and *ITGAD* (Figure 3; supplemental Figure 3; supplemental Table 11). Interestingly, GEP signatures and several genes associated with BCR–TLR–NF-κB and BRAF-MAPK signaling pathways and cell adhesion were hypomethylated and overexpressed. Conversely, cell-differentiation markers and methylated genes in cancer appeared hypermethylated and underexpressed (Figure 4; Table 1; supplemental Table 12).

Methylation profiling distinguishes HCL from other B-cell tumors

We then integrated gene expression and methylation data to compare HCL with SMZL and CLL. This analysis showed a marked overlap with the deregulated pathways identified in the comparison of HCL with post-GC B cells, suggesting a specific methylation-driven gene expression signature of HCL cells. A set of 245 genes was differentially methylated and expressed in HCL compared with SMZL and CLL. The top 10 hypermethylated and underexpressed genes were *LILRA4*, *SFTPB*, *TNFRSF13B*, *KCNN4*, *PMAIP1*, *CXCR5*, *TRAF5*, *TGIF1*, *FAM65B*, and *LILRB4*, whereas *RIN2*, *BTBD3*, *SPARCL1*, *SLITRK5*, *EMP1*, *CXADR*, *CAMK1*, *PLOD2*, *LRRC32*, and *CHN2* were hypomethylated and overexpressed (Figure 5; supplemental Figure 4; supplemental Table 13). Finally, when HCL methylation profiles were compared with those of CLL–VH3-21, 85 differentially methylated genes were differentially identified, because there were no publicly available GEP data for this subset of CLL. Among the top low-methylated genes we found *RAD50*, *FOXD1*, *RORA*, *CCNC*, and *WT1*, whereas *FCER1G*, *CCL2*, *NFKBIE*, *CD86*, and *MGMT* appeared hypermethylated (supplemental Table 13).

The gene expression signature of HCL includes B-cell survival pathways

Enrichment analysis revealed high expression of signaling pathways that are key to B-cell survival among the hypomethylated and overexpressed transcripts. These included integrin and CD40 signaling, MAPK (ERK, JNK) and RAS–RAF–MEK–ERK pathways, NF-κB activation upon TLR signaling, and B-cell activation mediated by the IKK complex. In accordance with the postulated HCL cell of origin, GC and pre-GC programs were methylated and repressed in HCL. Similarly, genes involved in transcription and the respiratory cascade, as well as genes harboring methylation marks, appeared more methylated and less expressed in HCL than in the other entities (Figure 6; supplemental Table 14).

Discussion

We have characterized the genome-wide DNA promoter methylation pattern of HCL and compared it with normal B-cell subsets and with other mature B-cell tumor entities (U-CLL, M-CLL, IGHV3-21 CLL, and SMZL). HCL had a distinct methylation pattern. The closest normal counterpart was post-GC B cells (low-maturity memory and intermediate-maturity memory B cell), along with MGZ B cells. The closest neoplastic entity was SMZL, which is in agreement with HCL and SMZL being morphologically and phenotypically similar, albeit distinct, tumor entities.

HCL is characterized by the presence of the BRAF V600E somatic mutation, which leads to constitutive BRAF–MEK–ERK pathway activation and represents an effective therapeutic target in patients.[1-5] However, BRAF inhibitors are unable to completely eradicate HCL,[2,3,6] suggesting that factors other than genetics may contribute to disease pathogenesis and behavior. The platform used in this study had a limited number of genes compared with the arrays currently available and was not associated with the gene-expression profile of the individual cases. However, we were still able to define the contribution of promoter methylation to the previously reported HCL gene expression signature,[32] identifying a set of hypomethylated and highly expressed genes associated with the BCR and the BRAF signaling pathways. This result supported the notion that promoter methylation is generally associated with repression of transcription and vice versa.[36]

Different methylation changes that we observed in HCL were consistent with the constitutive activation of the RAS–RAF–MEK–ERK pathway,[1-3] pointing to a permissive epigenetic landscape as a player in the upregulation of BRAF-related genes and, thus, participating in the specific biology of HCL. *RIN2*, encoding for a Ras effector that plays a role in the stimulation of GTPase activity,[37] was hypomethylated and overexpressed. Transcriptional targets of the Ras cascade, such as *EMP1*, encoding an integral tetraspan membrane protein,[38] were hypomethylated and overexpressed. There was hypomethylation and overexpression of *IGFR1*, which initiates a cascade of downstream signaling events leading to activation of the RAS/MEK/ERK pathway,[39] IGF-related signatures, and its direct target gene *SPARCL1*.[40] *CMKLR1* appeared hypomethylated and overexpressed in HCL. The protein product of *CMKLR1*, RARRES2, which induces cell proliferation by increasing phosphorylation of ERK1/2,[41] was also overexpressed. Hypermethylation of *CD151* may also cooperate with BRAF V600E somatic mutation in the RAS constitutive signaling of HCL patients, because the gene acts as a negative regulator of adhesion-dependent

Table 1. Methylation and gene expression profiles of pathologically relevant transcripts in HCL

						HCL vs post-GC B cells							
						Methylation profiling					GEP		
Pathway/process	Probe	CGI	Gene region	Enhancer	Symbol	Fold change*	*P* (Student *t* test)	*P* (adj. Student *t* test)†	M-value HCL	M-value post-GC B ceils	Fold change*	*P* (Student *t* test)	*P* (adj. Student *t* test)†
BCR–TLR–NF-κB signaling	cg14155397	NShore	TSS1500	noENH	MAP2K1	−2.130	.000	.000	−3.050	−0.920	0.929	.009	.031
	cg06827976	OpenSea	5′UTR	noENH	FGR	−1.812	.000	.000	0.026	1.838	1.821	.000	.000
	cg18508525	OpenSea	TSS1500	noENH	CD36	−1.502	.000	.000	1.179	2.681	1.555	.036	.040
	cg06618866	Island	TSS1500	noENH	TLR2	−1.201	.000	.000	−3.738	−2.536	1.332	.001	.007
	cg10862535	SShore	TSS200	noENH	PGLYRP1	−0.983	.002	.006	−2.536	−1.553	1.726	.036	.049
BRAF-MAPK signaling	cg05885720	OpenSea	TSS1500	ENH	EMP1	−3.927	.000	.000	−0.291	3.636	4.108	.000	.000
	cg17016000	OpenSea	TSS1500	ENH	RIN2	−3.497	.000	.000	−0.795	2.702	4.727	.000	.000
	cg05350879	OpenSea	TSS1500	noENH	SPARCL1	−3.120	.000	.000	−0.940	2.180	5.441	.000	.000
	cg00298951	OpenSea	TSS1500	ENH	CMKLR1	−2.828	.000	.000	−0.893	1.935	2.501	.000	.000
	cg14400118	NShore	1st exon	noENH	MMP2	−1.989	.000	.000	−3.606	−1.617	1.678	.000	.003
	cg01697865	NShore	TSS1500	noENH	IL10RA	−1.912	.000	.000	−3.059	−1.148	1.683	.000	.000
	cg05050341	SShore	TSS1500	noENH	ENG	−1.417	.000	.000	−0.270	1.147	2.239	.000	.000
	cg22736323	NShore	1st exon	noENH	PDGFRA	−1.370	.000	.000	−2.983	−1.613	3.007	.003	.013
	cg19853760	NShore	1st exon	noENH	LGALS1	−1.338	.000	.000	−1.105	0.233	2.248	.000	.000
Cell adhesion	cg02164442	OpenSea	Body	noENH	ITGAD	−2.469	.000	.000	−1.612	0.857	2.390	.000	.001
	cg05062178	Island	Body	noENH	ITGB5	−2.047	.000	.000	−3.632	−1.586	3.890	.000	.000
	cg12400041	SShore	Body	noENH	DST	−1.389	.000	.000	0.701	2.090	4.978	.000	.000
	cg20795401	NShore	TSS1500	noENH	ITGA6	−1.356	.000	.000	−3.186	−1.830	3.200	.000	.000
	cg14568338	Island	TSS1500	noENH	IGF1R	−1.115	.000	.000	−4.106	−2.991	1.324	.000	.003
B-cell differentiation and development	cg15645309	OpenSea	TSS200	noENH	BATF	1.463	.000	.000	−1.757	−3.219	−2.577	.000	.000
	cg04387658	OpenSea	Body	noENH	CD86	1.569	.000	.000	1.517	-0.052	−1.947	.000	.000
	cg20162076	OpenSea	TSS1500	noENH	LY86	1.679	.000	.000	1.014	−0.665	−1.341	.000	.002
	cg16280667	OpenSea	5′UTR	noENH	CXCR5	1.900	.000	.000	−0.752	−2.652	−3.672	.000	.000
	cg18152830	OpenSea	Body	noENH	TNFRSF13B	4.025	.000	.000	1.412	−2.613	−1.715	.000	.000
Methylated in cancer	cg25983380	Island	3′UTR	noENH	GNAS	0.828	.023	.047	−1.032	−1.860	−0.956	.007	.026
	cg24019564	Island	TSS1500	noENH	RUNX3	0.999	.000	.001	1.265	0.266	−1.013	.011	.039
	cg22375610	OpenSea	1st exon	ENH	APOBEC2	1.188	.000	.000	1.868	0.680	−1.151	.013	.043
	cg26201213	SShore	Body	noENH	MGMT	1.354	.000	.001	−0.837	−2.191	-0.994	.020	.059
	cg17489897	Island	5′UTR	noENH	PTEN	1.943	.000	.000	−3.831	−5.775	−1.082	.000	.001

Differentially methylated and expressed transcripts were selected by supervised comparison (moderated Student *t* test) of the methylation and gene expression profiles of HCL and post-GC B-cell subsets (MGZ, IoMBC, and intMBC, grouped as 1 pool). The annotation of methylation probes is detailed in the columns. Detailed information on the annotation of probes is available on the Illumina Web site. Gene region refers to the gene region with respect to the promoter, and the presence of an enhancer site (ENH) or not (noENH).

Body, between the ATG and stop codon, irrespective of the presence of introns, exons, TSSs, or promoters; N, upstream (5′) of CGI; Open Sea, outside CGI; S, downstream (3′) of CGI; Shelf, 2-4 kb from island; Shore, 0 to 2 kb from island; TSS200, 0 to 200 bases upstream of the transcriptional start site (TSS); TSS1500, 200 to 1500 bases upstream of the TSS; 3′UTR, between the stop codon and poly A signal; 5′UTR, within the 5′ untranslated region (UTR) between the TSS and the ATG start site.

*Fold change corresponding to the M-value difference (methylation) or to the log2 difference (gene expression) between HCL and post-GC B cells.

†The adjusted (adj.) *P* value refers to the Bonferroni correction of the nominal *P* value.

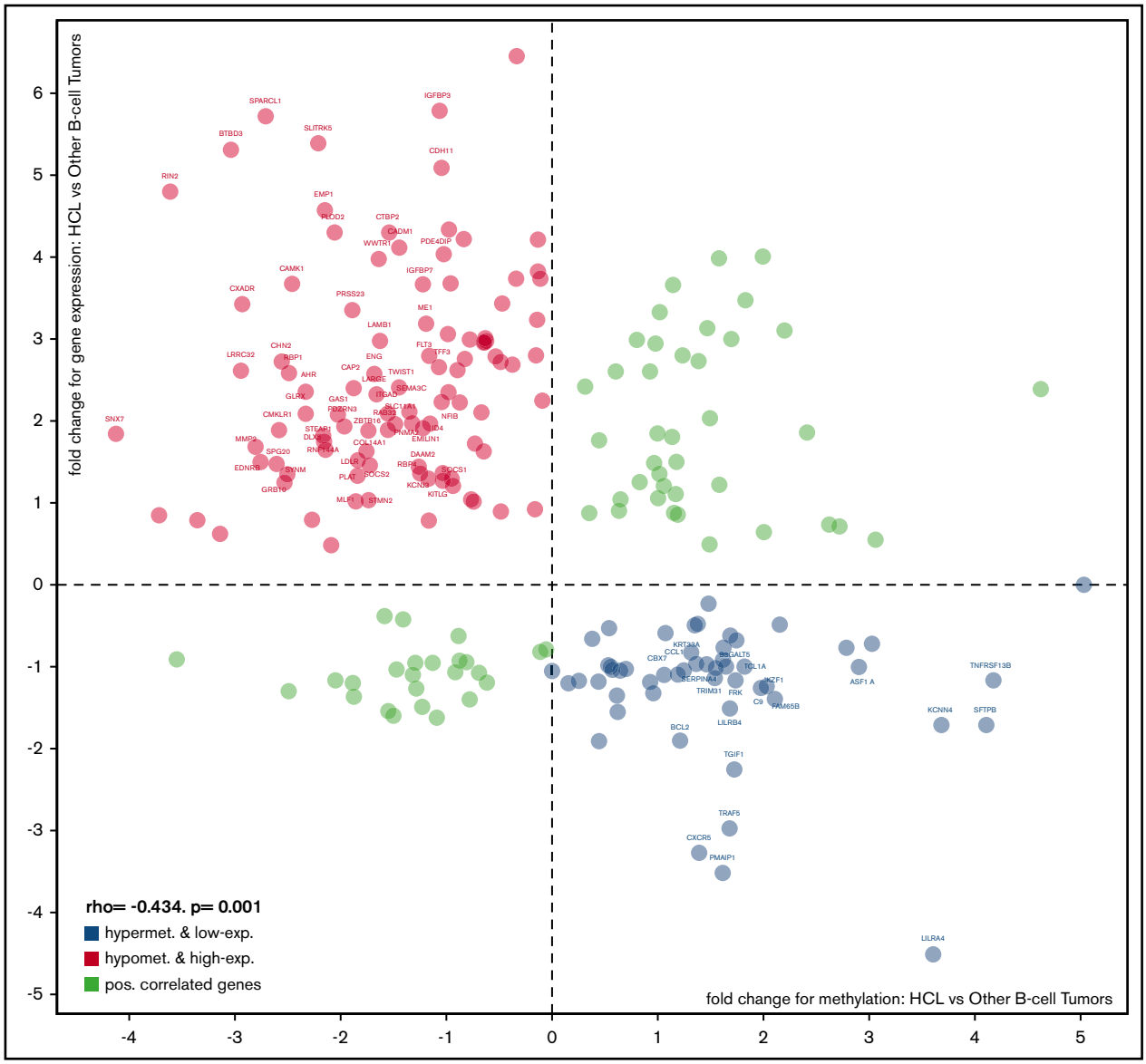

Figure 5. Integration of methylation and gene expression profiles of HCL and other tumor entities. Scatter plot on the differentially methylated or expressed genes (q value < 0.05; absolute difference of average M-values > 1.0 for methylation, and absolute $\log_2$ fold change >1.0 for gene expression). Δ of M-value is represented on the x-axis, whereas the y-axis represents $\log_2$ fold change in gene expression. Negatively correlated genes are labeled and highlighted in blue (hypermethylated and underexpressed) or in red (hypomethylated and overexpressed), whereas positively correlated genes are not labeled and are represented in light green. The ρ and P values correspond to Pearson's correlation for methylation and GEP fold changes.

activation of Ras.[42] *CHI3L2*, the most hypermethylated gene in HCL compared with other B-cell tumors, encodes for a component of the chitinase family that has been reported to be hypermethylated in RAS-activated cancer subtypes.[43] *VHL* is a tumor-suppressor gene that mediates degradation of the hypoxia-inducible factor, contributing to the activation of a series of pathways, including the RAS–RAF–MEK–ERK pathway,[44] which is constitutively active in HCL. Last, and consistent with this constitutive activation, a number of hypomethylated genes in HCL are likely to contribute to RAS signaling, including *MAP2K1*, *IL10RA*, *LAPTM5*, and *TRAF1*. Among these, *MAP2K1* and *IL10RA* also had a high expression in HCL. *MAP2K1* encodes for the BRAF-downstream kinase MEK1, and it is activated by somatic mutation in 50% of HCL-variant patients.[5,45] *IL10RA* is reported to promote survival upon ERK phosphorylation.[46]

Our current work also identified methylation patterns that may affect homing/migration and survival pathways of tumor cells. HCL is characterized by a gene expression signature[32] that appears to be inversely correlated with DNA promoter methylation, indicating the importance of methylation in gene expression control. Interestingly, the *CXCR5* promoter was methylated in our HCL samples. CXCR5 is a chemokine receptor for B cells, and its absence on HCL cells[47] might explain the lack of tropism of the tumor cells to the white pulp and to lymph nodes.

In this study, we found that antiapoptotic genes, including *TRAF5* and *TNFAIP8*, were hypermethylated. *TRAF5* and TNFAIP8

Figure 6. HCL shows distinct transcriptional and methylation signatures. Integrated methylation (A-B) and gene expression (C-D) profiles of HCL and post-GC B-cell subpopulations (A, methylation; C, gene expression profile) and of HCL and other B-cell tumors (B, methylation; D, gene expression profile). Heat maps show scores from ssGSEA (methylation or GEP). Supervised hierarchical clustering (Euclidean distance, complete linkage) of methylation profiles. The 4 main clusters on the rows comprise processes to be found in HCL with higher methylation and lower gene expression (1. High-M & Dn-Reg) or with lower methylation and higher gene expression (2. Low-M & Up-Reg) or positively correlated for methylation and gene expression (3. Positively correlated) or with no correlation (4. No correlated). *fc_met_norm* represents fold change in methylation between HCL and postGC B cells, *fc_met_tumor* represents fold change in methylation between HCL and other B-cell tumors, *fc_gep_norm* represents fold change in gene expression between HCL and post-GC B cells, and *fc_gep_tumor* represents fold change in gene expression between HCL and other B-cell tumors. Methylation profiling (histotype_Meth) included HCL, low- and intermediate-maturity memory B cells (loMat_postGC_Bcell and inMat_postGC_Bcell), splenic MGZ B cells (MGZ_Bcell), CLL samples (IGHV3-21$^+$ [CLL−VH3-2] and M-CLL and U-CLL IGHV), and SMZL. GEP (histotype_GEP) included HCL, memory B cells (postGC_Bcell), CLL samples (M-CLL and U-CLL IGHV), and SMZL.

expression is known to be downregulated in HCL.[32] *TRAF5* is a gene involved in the signal transduction of tumor necrosis factor–type receptors, including CD27, which is reduced by gene expression profile and not detectable by phenotype.[12] *TNFAIP8 (TIPE)* is a member of the tumor necrosis factor-α–induced protein family. Its repression protected hematopoietic cells from apoptosis,[48] and

TNFAIP8-deficient mice showed increased leukocyte infiltration.[49] Other genes, including cell-differentiation markers and known tumor-suppressor genes, appeared highly methylated in HCL. *O*-6-methylguanine–DNA methyltransferase, coded by *MGMT*, is involved in DNA repair and is often methylated in cancers, including lymphoid tumors.[50] *PRDM2* is also hypermethylated in leukemia and solid tumors, and its silencing induces high-grade B-cell lymphoma in mice.[51-53] *ENTPD1* encodes for the plasma membrane protein CD39 and may have diagnostic value, because it was hypermethylated in HCL compared with all CLL subsets (M-CLL, U-CLL, and CLL–VH3-21). Unsupervised and supervised analyses documented a highly methylated *TNFRSF13B* (*TACI*) and *MNDA* in HCL; indeed, these genes were proposed for the differential diagnosis of MZL vs B-cell tumor entities other than HCL.[54,55]

Among the genes that appeared hypomethylated in HCL, we found *FGF2* (fully nonmethylated across the series) and *FLT3*, which are known to be upregulated and might contribute to the bone marrow fibrosis that is characteristic of HCL.[32,56] Indeed, autocrine secretion of FGF2 by tumor cells is responsible for fibronectin production.[57] The ligand of FLT3, a potential therapeutic target in other leukemias,[58] is responsible for B-cell adhesion to fibronectin.[32] *RBBP4* and *SUZ12*, coding for components of the polycomb repressive complex 2, were hypomethylated, whereas genes silenced by methylation and transcripts harboring the trimethylation marks were methylated and repressed, pointing to the acquisition of a polycomb repression-associated methylator phenotype,[59] potentially linked to BRAF V600E mutation, at least in solid cancers.[60]

In conclusion, our data reveal that HCL differs from SMZL, CLL, and normal B cells and indicate that the HCL-specific methylation pattern affects pathways involved in the homing, migration, and survival of HCL cells.

Acknowledgments

This work was supported by the Hairy Cell Leukemia Foundation (New York, NY); the Nelia and Amedeo Barletta Foundation (Lausanne, Switzerland); Cancer Research UK (CRUK Centre grant C34999/A18087); the Southampton Cancer Research UK and NIHR Experimental Cancer Medicine Centres; the University of Southampton; Bloodwise (grants 16003, 14037, and 12021); the Keanu Eyles Haematology Fellowship for the Cancer Immunology Centre, University of Southampton; and the Gilead UK & Ireland Oncology Fellowship Programme 2016.

Authorship

Contribution: A.J.A. performed statistical analyses, interpreted data, and wrote the manuscript; A.R. performed DNA methylation profiling; G.C. reviewed and collected sample materials and diagnoses and interpreted data; I.K. and L.C. performed statistical analyses; D.R. and G.G. collected well-characterized tumor samples; M.K. and R.R. provided CLL methylation profiles; A.A.M., E.Z., and P.W.J. provided advice and interpreted data; C.C.O. analyzed and provided the profiles from the normal B-cell subsets; F.B. designed research, performed statistical analyses, interpreted data, and wrote the manuscript; F.F. designed research, collected and characterized tumor samples, interpreted data, and wrote the manuscript; and all authors approved the final manuscript.

Conflict-of-interest disclosure: The authors declare no competing financial interests.

ORCID profiles: L.C., 0000-0002-4606-0637; F.B., 0000-0001-5637-8983; F.F., 0000-0002-2211-1831.

Correspondence: Francesco Bertoni, Institute of Oncology Research, via Vincenzo Vela 6, 6500 Bellinzona, Switzerland; e-mail: francesco.bertoni@ior.usi.ch; and Francesco Forconi, Cancer Sciences Unit, University of Southampton, Cancer Research UK Centre, Somers Cancer Research Building, MP824, Southampton General Hospital, Southampton SO16 6YD, United Kingdom; e-mail: f.forconi@soton.ac.uk.

References

1. Grever MR, Abdel-Wahab O, Andritsos LA, et al. Consensus guidelines for the diagnosis and management of patients with classic hairy cell leukemia. *Blood*. 2017;129(5):553-560.
2. Falini B, Martelli MP, Tiacci E. BRAF V600E mutation in hairy cell leukemia: from bench to bedside. *Blood*. 2016;128(15):1918-1927.
3. Thompson PA, Ravandi F. How I manage patients with hairy cell leukaemia. *Br J Haematol*. 2017;177(4):543-556.
4. Tiacci E, Pettirossi V, Schiavoni G, Falini B. Genomics of hairy cell leukemia. *J Clin Oncol*. 2017;35(9):1002-1010.
5. Taylor J, Xiao W, Abdel-Wahab O. Diagnosis and classification of hematologic malignancies on the basis of genetics. *Blood*. 2017;130(4):410-423.
6. Tiacci E, Park JH, De Carolis L, et al. Targeting mutant BRAF in relapsed or refractory hairy-cell leukemia. *N Engl J Med*. 2015;373(18):1733-1747.
7. Dietrich S, Hüllein J, Lee SC, et al. Recurrent CDKN1B (p27) mutations in hairy cell leukemia. *Blood*. 2015;126(8):1005-1008.
8. Forconi F, Poretti G, Kwee I, et al. High density genome-wide DNA profiling reveals a remarkably stable profile in hairy cell leukaemia. *Br J Haematol*. 2008;141(5):622-630.
9. Rinaldi A, Kwee I, Young KH, et al. Genome-wide high resolution DNA profiling of hairy cell leukaemia. *Br J Haematol*. 2013;162(4):566-569.
10. Forconi F, Sozzi E, Rossi D, et al. Selective influences in the expressed immunoglobulin heavy and light chain gene repertoire in hairy cell leukemia. *Haematologica*. 2008;93(5):697-705.
11. Weston-Bell NJ, Hendriks D, Sugiyarto G, et al. Hairy cell leukemia cell lines expressing annexin A1 and displaying B-cell receptor signals characteristic of primary tumor cells lack the signature BRAF mutation to reveal unrepresentative origins. *Leukemia*. 2013;27(1):241-245.
12. Forconi F, Raspadori D, Lenoci M, Lauria F. Absence of surface CD27 distinguishes hairy cell leukemia from other leukemic B-cell malignancies. *Haematologica*. 2005;90(2):266-268.
13. MacLennan IC, Toellner KM, Cunningham AF, et al. Extrafollicular antibody responses. *Immunol Rev*. 2003;194(1):8-18.

14. Forconi F, Sahota SS, Raspadori D, et al. Hairy cell leukemia: at the crossroad of somatic mutation and isotype switch. *Blood*. 2004;104(10):3312-3317.

15. Forconi F, Sahota SS, Raspadori D, Mockridge CI, Lauria F, Stevenson FK. Tumor cells of hairy cell leukemia express multiple clonally related immunoglobulin isotypes via RNA splicing. *Blood*. 2001;98(4):1174-1181.

16. Queirós AC, Beekman R, Vilarrasa-Blasi R, et al. Decoding the DNA methylome of mantle cell lymphoma in the light of the entire B cell lineage. *Cancer Cell*. 2016;30(5):806-821.

17. Oakes CC, Martin-Subero JI. Insight into origins, mechanisms, and utility of DNA methylation in B-cell malignancies. *Blood*. 2018;132(10):999-1006.

18. Oakes CC, Seifert M, Assenov Y, et al. DNA methylation dynamics during B cell maturation underlie a continuum of disease phenotypes in chronic lymphocytic leukemia. *Nat Genet*. 2016;48(3):253-264.

19. Bröske AM, Vockentanz L, Kharazi S, et al. DNA methylation protects hematopoietic stem cell multipotency from myeloerythroid restriction. *Nat Genet*. 2009;41(11):1207-1215.

20. Kulis M, Heath S, Bibikova M, et al. Epigenomic analysis detects widespread gene-body DNA hypomethylation in chronic lymphocytic leukemia. *Nat Genet*. 2012;44(11):1236-1242.

21. Oakes CC, Claus R, Gu L, et al. Evolution of DNA methylation is linked to genetic aberrations in chronic lymphocytic leukemia. *Cancer Discov*. 2014;4(3):348-361.

22. Cahill N, Bergh AC, Kanduri M, et al. 450K-array analysis of chronic lymphocytic leukemia cells reveals global DNA methylation to be relatively stable over time and similar in resting and proliferative compartments. *Leukemia*. 2013;27(1):150-158.

23. Kanduri M, Cahill N, Göransson H, et al. Differential genome-wide array-based methylation profiles in prognostic subsets of chronic lymphocytic leukemia. *Blood*. 2010;115(2):296-305.

24. Queirós AC, Villamor N, Clot G, et al. A B-cell epigenetic signature defines three biologic subgroups of chronic lymphocytic leukemia with clinical impact. *Leukemia*. 2015;29(3):598-605.

25. Swerdlow SH, Campo E, Harris NL, et al, eds. WHO Classification of Tumours of Haematopoietic and Lymphoid Tissues. Vol 2. Revised 4th ed. Lyon, France: IARC Press; 2018.

26. Tiacci E, Schiavoni G, Forconi F, et al. Simple genetic diagnosis of hairy cell leukemia by sensitive detection of the BRAF-V600E mutation. *Blood*. 2012;119(1):192-195.

27. Rinaldi A, Mensah AA, Kwee I, et al. Promoter methylation patterns in Richter syndrome affect stem-cell maintenance and cell cycle regulation and differ from de novo diffuse large B-cell lymphoma. *Br J Haematol*. 2013;163(2):194-204.

28. Bibikova M, Le J, Barnes B, et al. Genome-wide DNA methylation profiling using Infinium assay. *Epigenomics*. 2009;1(1):177-200.

29. Fortin JP, Triche TJ Jr, Hansen KD. Preprocessing, normalization and integration of the Illumina HumanMethylationEPIC array with minfi. *Bioinformatics*. 2017;33(4):558-560.

30. Leek JT, Storey JD. Capturing heterogeneity in gene expression studies by surrogate variable analysis. *PLoS Genet*. 2007;3(9):1724-1735.

31. Smyth GK. Limma: linear models for microarray data. In: Gentleman R, Carey V, Dudoit S, Irizarry R, Huber W, eds. Bioinformatics and Computational Biology Solutions using R and Bioconductor. New York, NY: Springer; 2005:397-420

32. Basso K, Liso A, Tiacci E, et al. Gene expression profiling of hairy cell leukemia reveals a phenotype related to memory B cells with altered expression of chemokine and adhesion receptors. *J Exp Med*. 2004;199(1):59-68.

33. Subramanian A, Tamayo P, Mootha VK, et al. Gene set enrichment analysis: a knowledge-based approach for interpreting genome-wide expression profiles. *Proc Natl Acad Sci USA*. 2005;102(43):15545-15550.

34. Hänzelmann S, Castelo R, Guinney J. GSVA: gene set variation analysis for microarray and RNA-seq data. *BMC Bioinformatics*. 2013;14(1):7.

35. Seifert M, Küppers R. Determining the origin of human germinal center B cell-derived malignancies. *Methods Mol Biol*. 2017;1623:253-279.

36. Jones PA. Functions of DNA methylation: islands, start sites, gene bodies and beyond. *Nat Rev Genet*. 2012;13(7):484-492.

37. Saito K, Murai J, Kajiho H, Kontani K, Kurosu H, Katada T. A novel binding protein composed of homophilic tetramer exhibits unique properties for the small GTPase Rab5. *J Biol Chem*. 2002;277(5):3412-3418.

38. Durgan J, Tao G, Walters MS, et al. SOS1 and Ras regulate epithelial tight junction formation in the human airway through EMP1. *EMBO Rep*. 2015;16(1):87-96.

39. Saegusa J, Yamaji S, Ieguchi K, et al. The direct binding of insulin-like growth factor-1 (IGF-1) to integrin alphavbeta3 is involved in IGF-1 signaling. *J Biol Chem*. 2009;284(36):24106-24114.

40. Chowdhury S, Wang X, Srikant CB, et al. IGF-I stimulates CCN5/WISP2 gene expression in pancreatic β-cells, which promotes cell proliferation and survival against streptozotocin. *Endocrinology*. 2014;155(5):1629-1642.

41. Zhang R, Liu S, Guo B, Chang L, Li Y. Chemerin induces insulin resistance in rat cardiomyocytes in part through the ERK1/2 signaling pathway. *Pharmacology*. 2014;94(5-6):259-264.

42. Sawada S, Yoshimoto M, Odintsova E, Hotchin NA, Berditchevski F. The tetraspanin CD151 functions as a negative regulator in the adhesion-dependent activation of Ras. *J Biol Chem*. 2003;278(29):26323-26326.

43. Holm K, Hegardt C, Staaf J, et al. Molecular subtypes of breast cancer are associated with characteristic DNA methylation patterns. *Breast Cancer Res*. 2010;12(3):R36.

44. Clark PE. The role of VHL in clear-cell renal cell carcinoma and its relation to targeted therapy. *Kidney Int*. 2009;76(9):939-945.

45. Waterfall JJ, Arons E, Walker RL, et al. High prevalence of MAP2K1 mutations in variant and IGHV4-34-expressing hairy-cell leukemias. *Nat Genet*. 2014; 46(1):8-10.

46. Hsu TI, Wang YC, Hung CY, et al. Positive feedback regulation between IL10 and EGFR promotes lung cancer formation. *Oncotarget*. 2016;7(15): 20840-20854.

47. Dürig J, Schmücker U, Dührsen U. Differential expression of chemokine receptors in B cell malignancies. *Leukemia*. 2001;15(5):752-756.

48. Woodward MJ, de Boer J, Heidorn S, et al. Tnfaip8 is an essential gene for the regulation of glucocorticoid-mediated apoptosis of thymocytes. *Cell Death Differ*. 2010;17(2):316-323.

49. Sun H, Lou Y, Porturas T, et al. Exacerbated experimental colitis in TNFAIP8-deficient mice. *J Immunol*. 2015;194(12):5736-5742.

50. Rossi D, Capello D, Gloghini A, et al. Aberrant promoter methylation of multiple genes throughout the clinico-pathologic spectrum of B-cell neoplasia. *Haematologica*. 2004;89(2):154-164.

51. Steele-Perkins G, Fang W, Yang XH, et al. Tumor formation and inactivation of RIZ1, an Rb-binding member of a nuclear protein-methyltransferase superfamily. *Genes Dev*. 2001;15(17):2250-2262.

52. Oshimo Y, Oue N, Mitani Y, et al. Frequent epigenetic inactivation of RIZ1 by promoter hypermethylation in human gastric carcinoma. *Int J Cancer*. 2004; 110(2):212-218.

53. Shimura H, Mori N, Wang YH, Okada M, Motoji T. Aberrant methylation and decreased expression of the RIZ1 gene are frequent in adult acute lymphoblastic leukemia of T-cell phenotype. *Leuk Lymphoma*. 2012;53(8):1599-1609.

54. Arribas AJ, Gómez-Abad C, Sánchez-Beato M, et al. Splenic marginal zone lymphoma: comprehensive analysis of gene expression and miRNA profiling. *Mod Pathol*. 2013;26(7):889-901.

55. Kanellis G, Roncador G, Arribas A, et al. Identification of MNDA as a new marker for nodal marginal zone lymphoma. *Leukemia*. 2009;23(10):1847-1857.

56. Shapshak P. Molecule of the month, PDE4DIP. *Bioinformation*. 2012;8(16):740-741.

57. Aziz KA, Till KJ, Chen H, et al. The role of autocrine FGF-2 in the distinctive bone marrow fibrosis of hairy-cell leukemia (HCL). *Blood*. 2003;102(3): 1051-1056.

58. Kindler T, Lipka DB, Fischer T. FLT3 as a therapeutic target in AML: still challenging after all these years. *Blood*. 2010;116(24):5089-5102.

59. Schlesinger Y, Straussman R, Keshet I, et al. Polycomb-mediated methylation on Lys27 of histone H3 pre-marks genes for de novo methylation in cancer. *Nat Genet*. 2007;39(2):232-236.

60. Hinoue T, Weisenberger DJ, Lange CP, et al. Genome-scale analysis of aberrant DNA methylation in colorectal cancer. *Genome Res*. 2012;22(2): 271-282.